Foliage Profiles from Ground Based Waveform and Discrete Point Lidar

J.L. Lovell[1], D.L.B. Jupp[2], E. van Gorsel[2], J. Jimenez-Berni[2], C. Hopkinson[3] & L. Chasmer[4]

[1]CSIRO Marine and Atmospheric Research, Hobart, Australia, Jenny.Lovell@csiro.au
[2]CSIRO Marine and Atmospheric Research, Canberra, Australia
[3]Applied Geomatics Research Group, Lawrencetown, Canada
[4]Wilfrid Laurier University, Waterloo, Canada

Abstract

Terrestrial lidar systems provide a means to characterise the structure of a forest canopy. Their use to measure foliage area volume density depends on the ability to account for sampling effects and intensity calibration of the instrument. This paper presents a theoretical framework for the unbiased calculation of foliage amount using a waveform recording lidar instrument to simulate point cloud data. The method is initially based on the hemispherical scan configuration of the instrument, but is generalised to be applied to point cloud data in a generic coordinate system. The theory is tested with the simulated point cloud data as well as data from a commercial instrument. Foliage profiles from the instruments are found to be consistent.

1. Introduction

Leaf area index (LAI) and foliage area volume density (FAVD) are important quantities in the study of the structure and function of canopies e.g. light interception, respiration, transpiration, photosynthesis in multi-layer canopies all depend on these. While a few options exist for ground-based measurement of LAI, profiles of FAVD are more difficult as measurements are needed throughout the height of the canopy. This has been done successfully from the air with both lidar (e.g. Lefsky *et al*. 1999) and radar (Imhoff *et al*. 2000) but these methods often require on-ground calibration. Airborne instruments are also limited in the range of angular sampling and ability to sense structure through the full depth of a dense canopy. This is where ground-based lidar is an attractive option.

Parker *et al*. (2004) used a simple laser rangefinder to sample vertical gap probabilities along a transect and thus calculated vertical foliage profiles. Takeda *et al* (2005, 2008) also used a simple rangefinder system, but incorporated a 2-axis scan platform to allow angular sampling of the canopy. Their measurements of plant area density within gridded volume elements (voxels) resulted in plant area indices that reflected seasonal variation in the canopy, but significantly overestimated the actual amount of plant material. Hosoi and Omasa (2006) acquired multiple high resolution scans of single trees and used a ray tracing method to calculate contact frequency within voxels. From this they derived profiles of leaf area density which were validated against stratified clipping. Van der Zande *et al*. (2008) extended the Hosoi and Omasa (2006) methodology in a simulation study with virtual forest stands.

Jupp *et al*. (2009) have presented a method for estimating LAI profiles using a full-waveform ground-based lidar system. The terrestrial lidar system (TLS) used in the study was the Echidna® validation instrument (EVI) which has the advantage of scanning the full upper hemisphere with no gaps in laser illumination. The geometry of the scan (zeniths and azimuths of the outgoing beams) is also recorded along with the intensity profile of all target reflections.

In TLS that record discrete target locations, there is still the potential to estimate foliage amount and distribution provided sufficient information is recorded to characterise the geometry of the scan pattern and the intensity of the returns. In this paper, we summarise the method of Jupp *et al* (2009) and develop an equivalent method using discrete point lidar data, based on the polar geometry of the EVI scan. We then develop a voxel-based method for the calculation of the foliage amount per voxel using discrete point lidar data in a general coordinate system. We use a single EVI scan to illustrate the way in which waveform-based foliage profile method can be modified for use with discrete point data and then use the same data to test the voxel-based method. Scans of the same site using a discrete-point TLS system are also used to test the voxel method.

2. Theory

Jupp *et al*. (2009) present a method of estimating LAI profiles using a vertically resolved gap probability distribution, P_{gap}.

$$P_{gap}(\theta, z) = e^{-G(\theta)L(z)/\cos\theta} \tag{1}$$

where θ is zenith angle, z is height, $G(\theta)$ is the Ross G-function (Ross, 1981) and L is LAI. Provided with an estimate of $P_{gap}(\theta, z)$, the profile of leaf area can be calculated and thus the foliage area volume density which is the derivative of $L(z)$.

We now explore how P_{gap} can be estimated from TLS data, first following the Jupp *et al*. (2009) method using EVI data, then modifying this for application to discrete point data.

2.1 Hemispheric Waveform Method

The EVI waveform data processing uses a quantity called apparent reflectance. This is the reflectance of a diffuse target filling the beam of the instrument that would return the same intensity as recorded from the actual target. For a waveform recorded at zenith angle, θ, over ranges, r, it has the form

$$\rho_a = \frac{I(\theta, r)R^2}{K(R)\Phi_0} \tag{2}$$

where I is the range-dependent recorded intensity, R is the range to the target, $K(R)$ is a calibration function associated with the geometry of the receiver optics and Φ_0 is the energy of the outgoing pulse. Integrating ρ_a over range provides a step-wise reduction in the power of the outgoing signal brought about by hits on single or multiple targets. This is related to P_{gap} by

$$I_a(\theta, r) = 1 - p(\theta, g)\left(1 - P_{gap}(\theta, r)\right) \tag{3}$$

where I_a is the integral of ρ_a, g is the distribution function for facet directions of the targets and p is the mean phase function for the varying facets. Jupp *et al*. (2009) take the phase function as the square of the Ross G-function. In general, the phase function is unknown and if possible should be estimated from the data. Jupp *et al*. (2009) use an initial assumption of p=1 and then identify two thresholds in the calculated P_{gap} relating to (i) the maximum P_{gap} value for targets

that fully extinguish the beam (hard target) and (ii) the maximum P_{gap} value for targets that partially extinguish it (soft target), above which all samples are assume to be true gaps. These are used to scale the P_{gap} in a similar way to the two level separation of gap and vegetation that can be done in hemispherical photograph analysis (Leblanc *et al*., 2005).

The value of P_{gap} calculated from a single waveform is a realisation of an actual gap, rather than a probability, therefore it is necessary to average the measured values over some spatial region in order to estimate the underlying probability distribution. Using EVI data, it is convenient to average over a ring or sector between zenith angle limits. Jupp *et al*. (2009) describe a method for calculation of a mean foliage profile from zenith-ring averages of P_{gap}. The method uses a ratio of cumulative foliage area ($L(z)$) relative to LAI to provide a profile largely independent of clumping. The range-based zenith-ring averaged P_{gap} data are resampled onto a consistent height axis, z and the cumulative LAI profile is defined by

$$\frac{L(z)}{LAI} = \frac{\log P_{gap}\left(\bar{\theta}, z\right)}{\log P_{gap}\left(\bar{\theta}, H\right)} \tag{4}$$

where H is the height of the canopy and the notation $\bar{\theta}$ indicates that the data are averaged over a range of zenith angles, rather than a mean angle. The foliage area volume density profile is then

$$f(z) = LAI \frac{\partial}{\partial z}\left(\frac{\log P_{gap}\left(\bar{\theta}, z\right)}{\log P_{gap}\left(\bar{\theta}, H\right)} \right). \tag{5}$$

In these equations the value of LAI can also be estimated from the EVI data either from data near the zenith angle $\theta \approx 57.5^{\circ}$ or from a simple linear canopy model as shown by Jupp *et al*. (2009). The profiles are calculated for a number of zenith rings i.e. different values of $\bar{\theta}$, and then a mean profile is calculated by weighting each profile according to the solid angle subtended by the ring. Jupp *et al*. (2009) note that the measurements based on the EVI data do not separate plant material into leaf and stem. Thus the quantities calculated are in fact plant area index and plant area volume density, however we will maintain the notation of the previous work. This paper is concerned with the comparison of methods applied to two sets of lidar data so the distinction between plant and leaf is unnecessary in this case.

2.2 Hemispheric Discrete Point Method

Waveform EVI data can be converted to (x, y, z) point data by applying a filter based on the known shape of the outgoing laser pulse. There may be single or multiple targets identified from each waveform. The output records from the conversion process include x, y, z, coordinates, apparent reflectance, outgoing zenith and azimuth angles, the number of hits from the shot and the hit number of the particular point. There is also a record of shots for which no hits were detected i.e. sky gaps. This point cloud data retains the geometric and sampling advantages of the waveform data but also allows us to demonstrate that it is possible to produce equivalent foliage profile information from discrete data.

We now develop a method to calculate P_{gap} from the point cloud data. It is again useful to accumulate data over zenith rings or sectors. We first define an unscaled P_{gap} term, *pg*:

$$pg\left(\bar{\theta},r\right)=1-P_{hit}\left(\bar{\theta},r\right)=1-\frac{\sum_{0}^{r}hit_{w}}{n_{shot}vol} \quad (6)$$

where hit_w is a weighting value for each hit up to range, r, n_{shot} is the total number of outgoing pulses in the zenith range and *vol* is the illuminated volume in the zenith range. The weighting of the hits is either the apparent reflectance value of the target points, or a weighting defined by the number of hits from a single shot (e.g. points recorded from a waveform with n hits detected would each be assigned a weight of 1/n).

The illuminated volume, *vol*, is a factor that is necessary to take into account the obscuration of some regions by targets at closer range to the instrument. It can be calculated from the point cloud data by identifying the last hit from each shot and calculating the volume contained within these final hits.

The quantity *pg* needs to be scaled to account for the phase effect. We do this by applying a simple linear scale defined to rescale the quantity to achieve a value of P_{gap}=1 for true sky gaps.

$$P_{gap}\left(\bar{\theta},r\right)=1-\frac{pg\left(\bar{\theta},r\right)\left(1-skyratio\right)}{\left(1-pg\left(\bar{\theta},r_{\max}\right)\right)} \quad (7)$$

where *skyratio* is defined within the same zenith ring or sector as the ratio of the number of shots where no hits were recorded, to the total number of shots and r_{max} is the maximum range covered by the data.

For each of the zenith rings, we resample the P_{gap} onto a consistent height axis to give $P_{gap}\left(\bar{\theta},z\right)$ which can be used in equations (4) and (5) in the same way as the waveform-based P_{gap}.

2.3 Voxel Method

In order to develop a more general algorithm that can be applied to point data from different TLS instruments, we now develop the theory from the perspective of voxels. We define foliage area volume density, $f\left(\theta,\phi,r\right)$ for a voxel at polar coordinates (θ,ϕ,r) such that

$$\int_{0}^{r} f\left(\theta,\phi,r\right)dr' = L\left(z\right)\Big/\cos\theta \quad (8)$$

where $z=r\cos\theta$. Consider now the illumination of the foliage elements in this voxel by a laser which has passed through the canopy to this point with a gap probability, $P_{gap}\left(\theta,\phi,r\right)$. The observed apparent reflectance of the voxel, ρ_a can be expressed as

$$\rho_a = G\left(\theta\right)p\left(g,\theta\right)P_{gap}\left(\theta,\phi,r\right)f\left(\theta,\phi,r\right)\rho_t . \quad (9)$$

The total effective area of objects in the voxel is $f(\theta,\phi,r)$ multiplied by the volume of the voxel. It is useful at this point to generalise the expressions by converting to Cartesian coordinates, thus

$$LA_V = \frac{V}{G(\theta)\,p(g,\theta)} \frac{\rho_a(x,y,z)}{P_{gap}(x,y,z)} \tag{10}$$

Where LA_V is the leaf area within the voxel and V is the volume of the voxel. If we divide by the base area of the voxel, we obtain an expression for a leaf area index of the voxel:

$$L_V = \frac{h_z}{G(\theta)\,p(g,\theta)} \frac{\rho_a(x,y,z)}{P_{gap}(x,y,z)} \tag{11}$$

where h_z is the height of the voxel. This can be summed vertically to obtain canopy LAI above the base of the voxel. This provides an algorithm to calculate leaf (or plant) area in voxels given the apparent reflectance returned from that voxel and an estimate of the gap probability at that point in the canopy. This expression is valid only for voxel that are illuminated i.e. not obscured from the instrument due to closer canopy elements. It is therefore best applied in situations where there are multiple scans that provide consistent illumination and overcome obscuration. Where there is incomplete illumination, equation (11) will provide an approximation to the true foliage area volume density sampled according to the illumination of the volume. If the illuminated volume can be characterised, a correction could be made, however it has not been attempted at this stage.

3. Data Collection

Data were collected from 8-10 December 2009 in a tall eucalypt forest near Tumbarumba, Australia (35°36'42"S, 148°06'29"E) at the location of the Tumbarumba FLUXNET site (Leuning *et al*., 2005). The forest has a 2-layer canopy and significant ground cover of shrubs and grasses. Terrestrial lidar data were collected with the EVI waveform lidar and an ILRIS discrete return system.

The EVI dataset is a single hemispherical scan. The EVI lidar is designed to capture data from at least the full upper hemisphere in a single acquisition and cover the field of view with no gaps in laser illumination. The laser operates at a wavelength of 1064 nm with a pulse repetition frequency of 2 kHz. The exiting laser beam has a diameter of 29 mm and the adjustable beam divergence was set at 5 mrad. In contrast to most terrestrial lidar systems that record a single range for each laser shot, the EVI records the light reflected from objects along the laser path as a waveform sampled at 2 GSs^{-1}, or one sample every 7.5 cm of range from the instrument. The direction (zenith and azimuth) of the outgoing laser pulse are also recorded. Further details of the EVI instrument are given by Jupp *et al*. (2005).

ILRIS is a tripod-mounted eye safe lidar imaging system manufactured by Optech Incorporated, Toronto, Canada. The instrument emits 2000 laser shots per second across a horizontal and vertical field of view of 50° and operates at a near infra-red wavelength of 1550 nm. The range of either the first or last pulse reflected back to the unit from each shot emitted can be stored. Ranges of up to and over 1 km can be recorded. The scan settings can be user configured either for speed of data collection or for high data density. For example, a typical scene of 1.2 – 1.8 million points will be acquired in 10 – 15 minutes. The beam divergence of the pulse is 0.2 mrad. At distances of 50 m away from the sensor, the spot size is approximately 1 cm in

diameter. Spot spacing is a function of the user configurable horizontal and vertical field of view and distance from the sensor. However, a nominal spacing at a 50 m range would also be on the order of 1 cm. ILRIS scans were undertaken at the same location as the EVI as well as from the four cardinal directions looking in towards the EVI location at a distance of approximately 80-100 m as illustrated in Figure 1. At each of these locations, a ground-parallel and an upwardly inclined canopy-viewing scan were collected, recording the last return for each pulse. Each ILRIS position was approximately positioned using a dGPS rover mounted on top of the sensor head. The dGPS positions were differentially corrected to a base station less than 10 km away. However, given the GPS occupations were under canopy and the receiver used was a single frequency (L1 only), only one scan was positioned to the cm level. The remaining locations are accurate to within approximately 0.5 m.

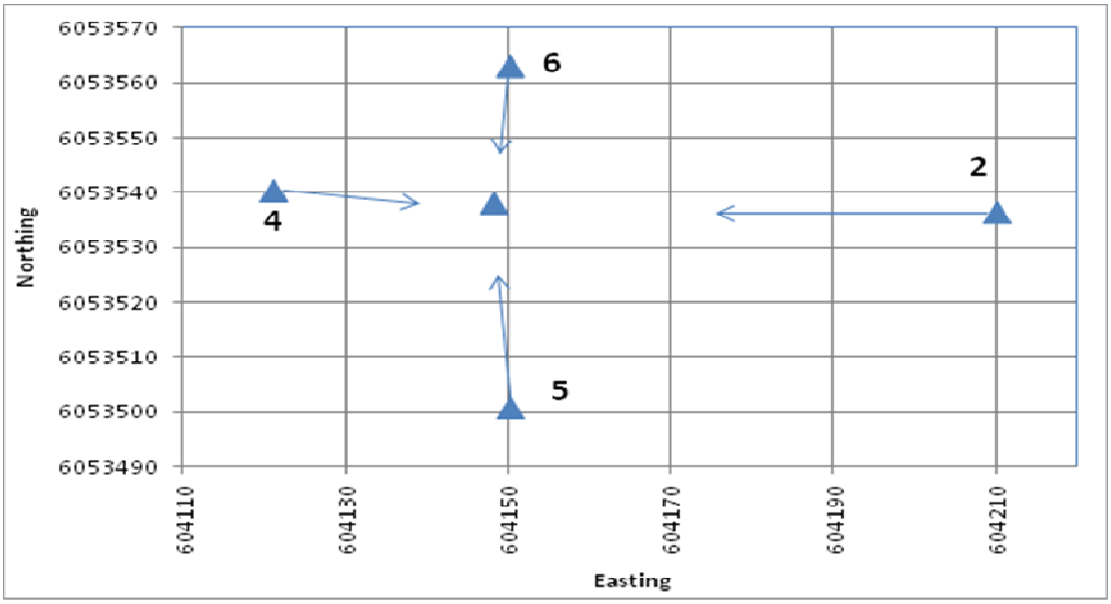

Figure 1: ILRIS scan configuration with 4 scan locations looking into centre of the EVI scan location from north, east, south and west ILRIS scan locations. Each ILRIS scan location has two scans: one parallel with ground and another inclined vertically and aimed into the canopy.

The images in Figure 2 show a comparison of the two datasets. The ILRIS data are shown for a square subset ±40 m from the EVI location as that data covers a larger area and is more dense. The two images are approximately aligned. It is clear that the single viewpoint of the EVI data suffers from occlusion in some areas e.g. there are sectors occluded by the trunks of central trees. These are evident to some extent in the ILRIS data, but are mostly filled by data from different view directions. This can be seen in the Figure 2 images where there is a dark sector in the foreground of the EVI image that is filled with low vegetation in the ILRIS image.

4. Demonstration of Results

The EVI waveform data gives us the flexibility to test the theoretical methods using a single dataset, processed and sampled in varying ways. The first and baseline foliage profile that we derived is the waveform-based profile following the method of Jupp *et al*. (2009). This is shown in Figure 3a as the black line. It shows a 2-layer canopy as expected and sums to an LAI value of 2.4 which is comparable to published values for this site (Leuning *et al*. 2005).

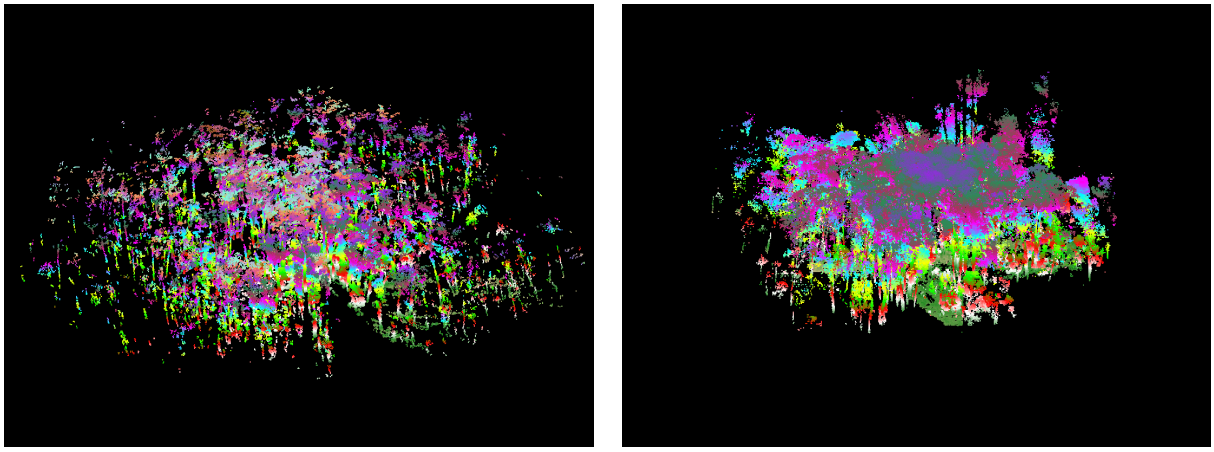

Figure 2: EVI data (left) shown as a point cloud derived from the waveform data and a subset of the ILRIS point cloud (right). The extent of the EVI data is approximately 50 m from the centre of the plot. The ILRIS data has been subset to 80 m x 80 m. The maximum tree height is approximately 40 m. Colours represent height.

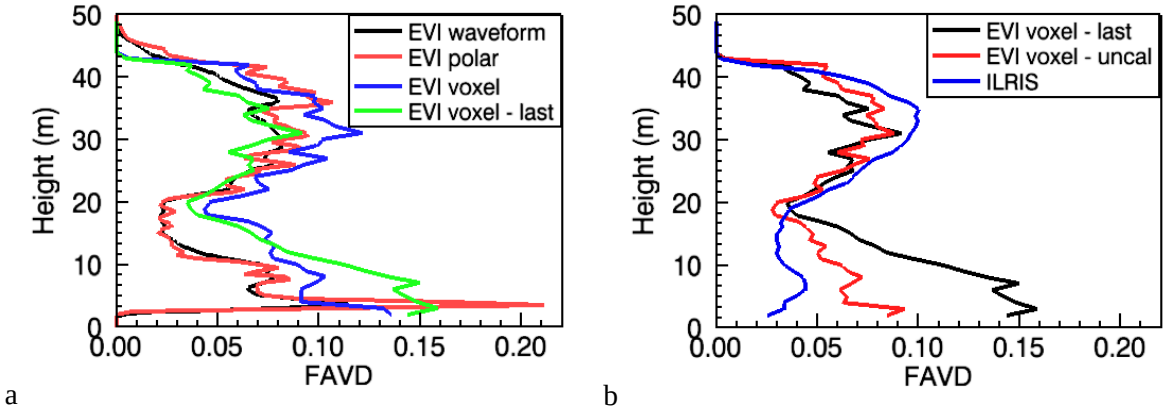

a b

Figure 3: Comparison of foliage profiles derived using the different methods applied to EVI data (left) and ILRIS data foliage profiles compared with the EVI last hit data (right).

The EVI data were filtered based on the known shape of the outgoing laser pulse, to produce discrete point data. This process records all detected targets for each shot and also maintains a record of the outgoing pulse geometry for all shots, including those that do not return any significant hits. This data can then be processed using equation (7) to produce gap probabilities for a number of equal zenith angle rings. These are then used in the same way as the waveform-based P_{gap} results to calculate a mean foliage profile over all zenith angles (equation (5)). This process has been done using two kinds of weighting in equation (6). The primary method of weighting (shown in red in Figure 3a) is the apparent reflectance calculated for the point. The alternative, which is of use where calibrated intensity data are not available, is to weight points according to the number of hits recorded in the shot. This produces a similar result and is not shown here. The point cloud result is not as smooth a curve as the waveform result. This may be due at least in part to the calculation of the illuminated volume which is based on the assumption that all final hits fully extinguish the beam. This is not always true and will introduce some error into the calculation.

The voxel method described in Section 2.1 takes a different approach, calculating the foliage area volume density represented by each hit and assigning this to the appropriate spatial voxel in a grid. Where multiple points fall into a voxel, the average value is used. The theory has been

described for multiple-return lidar data, but can also be applied to single returns. This is illustrated by application to the full EVI point cloud as well as a reduced point cloud of just the last returns from each laser shot. These are shown as the blue and green lines respectively in Figure 3a.

The ILRIS point cloud data are last return data and although there is an intensity value recorded, it is not calibrated. We have therefore treated each point with equal weighting and used an approximated value for the apparent reflectance to generate a foliage profile of close to the same magnitude as the EVI data. This is shown in Figure 3b (blue curve) compared with the EVI last hit profile (black) as well as a profile calculated from the EVI last hit data with apparent reflectance approximated to a constant in the same way as the ILRIS data.

The foliage profiles in Figure 3 all show the 2-layer characteristic of the canopy. There is significantly more variation in the foliage amount seen in the understorey layer than in the upper canopy. The voxel-based methods produce larger foliage volumes than the waveform and polar point cloud method. This is probably due to the fact that non-illuminated volumes have been disregarded in this study.

5. Discussion

Simulation of discrete point lidar data from the EVI waveform data has provided a means to test the theory presented here. The polar point cloud method was shown to give very similar results to the waveform method. Thus we are confident that given the right geometric and radiometric information, terrestrial lidar point cloud data can be successfully used to map foliage area volume density within a canopy.

Comparing the results of the multiple scan ILRIS dataset with the equivalent calculations from the EVI data shows some differences that may be associated with the more complete illumination achieved with multiple scans. The EVI profiles from last hits (black and red lines in Figure 3b) show a much larger volume of foliage in the lower canopy than is seen in any of the other profiles. This is not evident in the ILRIS scan and is probably due to the extra stability provided by the multiple scan locations. The EVI instrument was positioned close to some shrubs and trunks which dominate the lower parts of the foliage profile. The trunks in particular produce high intensity reflections. It is clear that this is a dominant effect since the uncalibrated EVI voxel method, where each point is assigned the same reflectance, produces a profile with less material in the understorey. Deploying the EVI instrument at more than one location and combining the information from multiple scans would help to overcome such bias.

The voxel-based method shows promise and has produced results that are reasonably consistent with the waveform data. However there are aspects of the method that require further investigation. In situations where the scan pattern does not provide complete illumination, the compensation for non-illuminated volume needs to be investigated. If the scan pattern of the lidar is known, then it is possible to map which voxels are illuminated. However, a simple adjustment according to the volume illuminated may not provide the solution because the patterns of illumination are related to the distribution of foliage elements and thus there is inherent bias.

Acknowledgements

We are grateful to Darius Culvenor and Glenn Newnham for assistance with EVI operation and Vanessa Haverd for assistance with fieldwork and reviewing the manuscript.

References

Hosoi, F. and Omasa, K., 2006. Voxel-based 3-D modelling of individual trees for estimating leaf area density using high-resolution portable scanning lidar *IEEE Transactions on Geoscience and Remote Sensing*, 44 (12), 3610-3618.

Imhoff, M.L., Johnson, P., Holford, W., Hyer, J., May, L., Lawrence, W. and Harcombe, P., 2000. BioSAR™: an inexpensive airborne VHF multiband SAR system for vegetation biomass measurement. *IEEE Transactions on Geoscience and Remote Sensing*, 38, 1458-1462.

Jupp, D.L.B., Culvenor, D.S., Lovell, J.L., Newnham, G.J., 2005. Evaluation and validation of canopy laser radar (LIDAR) systems for native and plantation forest inventory. Final Report prepared for the Forest and Wood Products Research and Development Corporation (FWPRDC: PN02.2902) by CSIRO. Available as CSIRO Marine and Atmospheric Research Paper 020 at http://www.cmar.csiro.au/e-print/open/cmar_rp020.pdf.

Jupp, D.L.B., Culvenor, D.S., Lovell, J.L., Newnham, G.J., Strahler, A.H., Woodcock, C.E., 2009. Estimating forest LAI profiles and structural parameters using a ground based laser called "Echidna®". *Tree Physiology*, 29, 171-181.

Leblanc, S.G., Chen, R., Fernandes, R., Deering, D.W. and Conley, A., 2005. Methodology comparison for canopy structure parameters extraction from digital hemispherical photography in boreal forests. *Agricultural and Forest Meteorology*, 129 (3–4), 187-207.

Lefsky, M.A., Cohen, W.B., Acker, A., Parker, G.G., Spies, T.A. and Harding, D., 1999. Lidar remote sensing of the canopy structure and biophysical properties of Douglas-Fir Western Hemlock forests. *Remote Sensing of Environment*, 70, 339-361.

Leuning, R., Cleugh, H.A., Zeglin, S.J., Hughes, D., 2005. Carbon and water fluxes over a temperate Eucalyptus forest and a tropical wet/dry savanna in Australia: measurements and comparison with MODIS remote sensing estimates. *Agricultural and Forest Meteorology*, 129 (3–4), 151–173.

Parker, G.G., Harding, J.H. and Berger, M.L., 2004. A portable LIDAR system for rapid determination of forest canopy structure. *Journal of Applied Ecology*, 41, 755-767.

Ross, J.K., 1981. *The radiation regime and architecture of plant stands.* Junk Publishers, The Hague, Netherlands.

Takeda, T., Oguma, H., Yone, T., Yamagata, Y. and Fujinuma, Y., 2005. Comparison of leaf area density measured by laser rangefinder and stratified clipping method. *Phyton – Annales Rel Botanicae*, 45 (4), 505-510.

Takeda, T., Oguma, H., Sano, T., Yone, T. and Fujinuma, Y., 2008. Estimating the plant area density of a Japanese larch plantation using a ground-based laser scanner. *Agricultural and Forest Meteorology*, 148 (3), 428-438.

Van der Zande, D., Jonckhere, I., Stuckens, J., Verstraeten, W.W. and Coppin, P., 2008. Sampling design of ground-based lidar measurements of forest canopy structure and its effect on shadowing. *Canadian Journal of Remote Sensing*, 34 (6), 526-538.